Completed Galactic Plane Analysis.

Peter Nemethy and Roman Fleysher
June 15, 2004

1 Introduction.

This note describes the completed analysis for the Milagro observation of TeV energy diffuse emission from the galactic equator, as a preliminary to, and detailed reference for, the galactic plane paper.

The term "diffuse gamma emission" must always be interpreted as meaning diffuse gamma plus unresolved-point source emission; by definition the two cannot be separated.

The analysis method is described in full detail in Roman's thesis (Ref.1) and in the methods paper by R. Fleysher et al. published in Ap. J. in March 2004 (Ref.2). We do not repeat these descriptions here but only highlight the most relevant features and later developments.

2 Data Sample, Event Selection, and Data Rejection.

The data sample analyzed is an exact three years of Milagro Data, from MJD1745 (July 19, 2000) to MJD 2839 (July 18, 2003). Event Selection cuts are:

- $NHIT > 50$ An explicit cut, beyond our hardware trigger.
- $TRIGGER-BIT = 2$ or $TRIGGER-BIT = 3$ from March 2002 on. Rejects low NHIT triggers.
- $NFIT > 20$.
- Zenith Angle $\theta < 50°$.
- Compactness Cut $X2 > 2.5$ (adjusted for major calib. change) for hadron rejection.
- Declination $10° < DEC < 60°$. Restricts to well-behaved anisotropy region.

Data run exclusions are made to avoid bad or variable-condition data:

- September PMT Repair Periods are excluded: MJD1806-1812, MJD2164-2170, and MJD2532-2541.
- Calibration Runs are Excluded.
- Special Runs are excluded. Example is low threshold running on Nov. 2002.

- Period of deep-water on cover is excluded (MJD2720-2744, March 2003).
- Periods with sudden rate change and/or sudden zenith distribution change are excluded. Example is a tripped low voltage power supply.
- Corrupt data, such as buffers with overwrites, are rejected.

3 The Basic Analysis.

- The background generation utilizes the earth's rotation, with time-swapping in an 8 hour time window, instead of the usual 2 hours, chosen to accommodate the finite source size of the galactic plane. The mathematical assumption underlying the method is that, in local coordinates x, the number of detected events can be factored into a time-independent acceptance shape G(x) and a time-varying rate R(t).
- Galactic Plane Exclusion. To maintain the statistical independence of the signal and background distributions, and to avoid the distortion of the generated background distribution from the presence of any galactic plane signal, a $\pm 7^\circ$ region in Galactic latitude around the Galactic equator is excluded in the background generation. To do this self-consistently, one has to find the unknown functions G(x) and R(t) for all of the traversed sky, that give rise to (i.e. best fits) the observed distributions outside the excluded region, then use these two functions for the time-swapping. In practice this is done by the iterative solution of coupled integral equations. For a detailed description of the method, see Ref.2. A monte-carlo simulation has shown the importance of the exclusion. A nonzero galactic signal is suppressed by about 25% if the galactic equator is not excluded, but is restored fully in the analysis with the galactic exclusion(Ref.2).
- Isotropy Assumption. The analysis is done in the approximation that the cosmic ray background is isotropic. See next section, however for a discussion of an anisotropy correction, applied to the output of this analysis.
- Zenith Breathing Correction. A significant repetitive diurnal variation in the zenith angle distribution has been observed in the data and parametrized as a correction function. The time swapping method has been modified to incorporate this functional dependence in the analysis (Ref.2).
- Sun-Moon exclusion. Although the sun and moon subtend a very small solid angle of order $10^{-4} ster.$, the signal strength of their shadow is 100%. The total deficit produced by each of these sources is of the same order of magnitude as the excess we search for. Therefore, two moving circles of radius 5° containing the sun and moon are excluded (Ref. 1).
- Milagro Inner Galaxy (IG). To search of for a possible galactic signal a single bin of galactic latitude from -5° to $+5^\circ$ and a galactic longitude from 40° to 100° is defined for the region of maximum Milagro exposure to the galactic equator nearest to the inner galaxy. A second region from 140° to 200° in longitude is defined as the Milagro Outer Galaxy(OG). Both

these regions have been redefined from those of Ref.1, because 20° to 40° and 200° to 220° have null exposure with our dec cut.

4 Results before and after Background Correction.

Fig. 1.(a) and 1 (b) show the exposure map and the significance map in galactic coordinates. The eye can see a narrow ridge of positive excess in the Inner Galaxy region. A single bin analysis gives an excess of 69,817 events over a background of 238,025,840 yielding a fractional excess of

$$FR = (2.93 \pm 0.73) \cdot 10^{-4} (4.0\sigma).$$

The error and significance are calculated with Eq.(3) of Ref. 2.

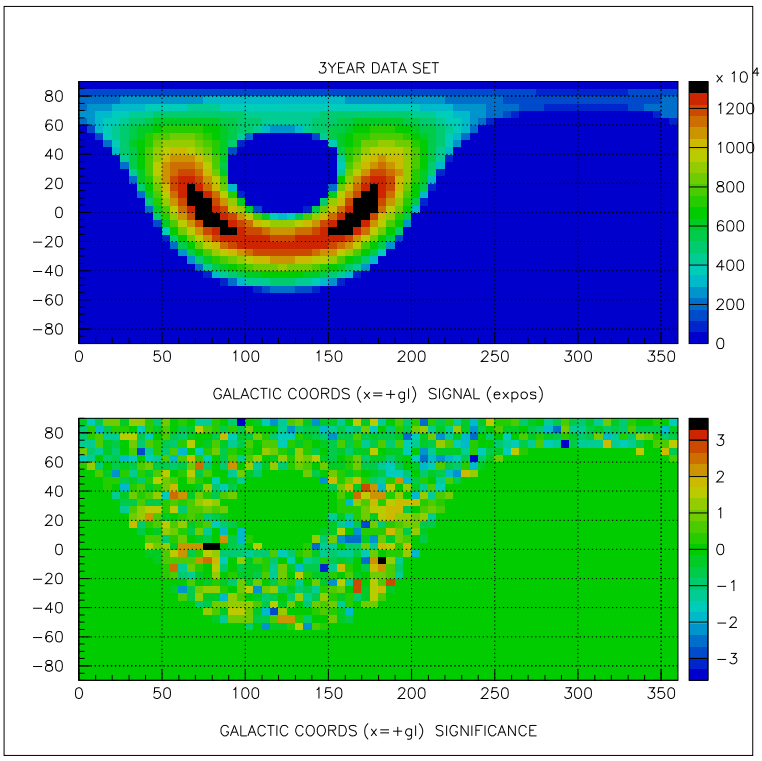

Fig. 1. (a) Exposure (b) Significance Map.

The broad (large angular scale) deficits and enhancements in the significance maps are interpreted as resulting from neglecting a small anisotropy of the cosmic ray background. Such an anisotropy was seen in a separate analysis(Ref.3) examining a forward-backward asymmetry in the data in the RA direction, as a function of sidereal time. It was seen to be described adequately by a 12parameter fit of the three longest harmonics, with amplitude and phase that are coherent but are allowed to vary linearly with declination. Fig. 2(b) shows the anisotropy map of X2-cut

data from that analysis. Such an anisotropy is expected to show up in the galactic plane analysis as some residual background with attenuated amplitudes during the moving 8 hour time-swapping windows generating the subtracted spectrum.

Although, in an ideal analysis, this anisotropy would be used as an input to the background calculation (see Ref.2), this was expected to require a very large increase in the needed computational time to reanalyze the data.[1] A different (approximate) method was chosen, by making the Ansatz that: The anisotropy induced modulations in the background-subtracted maps can be fitted with the same (coherent-in-dec) 3-harmonics, the same 12 parameters as the anisotropy. This Ansatz provides a functional form for the background correction.

The 12parameter fit to the subtracted distribution in RA DEC then provides the amplitudes and phases. To avoid the self-annihilation of the galactic ridge signal by the correction, it is again essential to exclude the Inner Galaxy region, or alternately the entire galactic equator (IG-OG) from the fit. Since no signal is expected (or seen) in the OG, we make the first of these choices (IGEX) but will also examine the second in estimating the systematic error of the correction.

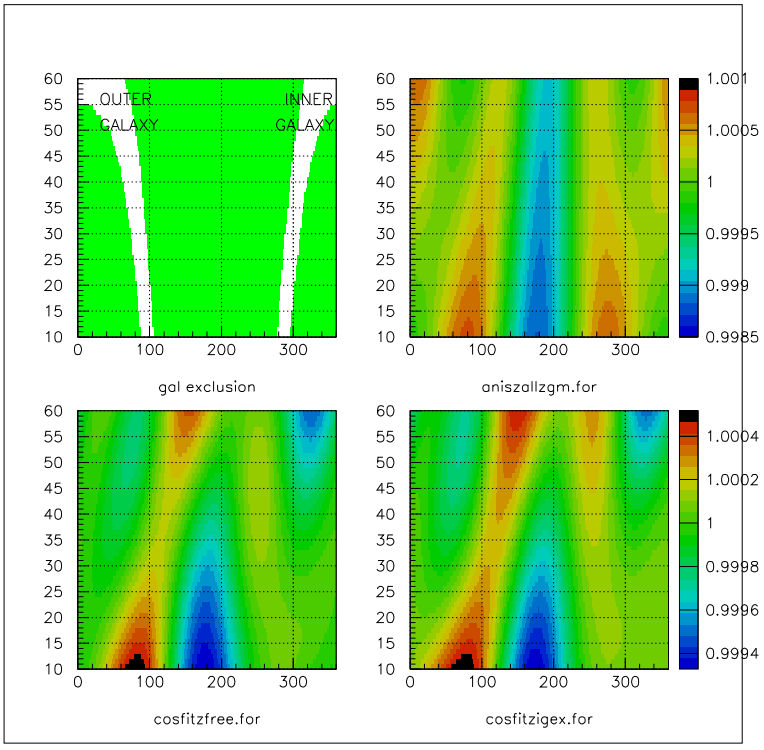

Fig. 2. (a)IG and OG. (b)Sky Anisotropy (c),(d) Background Correction (RA-DEC).

Fig. 2(a) shows the inner and outer galaxy exclusion regions, and Figs. 2(c) and 2(d) show the fitted RA-DEC correction functions, with IG or IG-OG excluded, respectively. The smilarity of the

[1]However, Roman is investigating an attempt to implement the ideal analysis without a prohibitive computational loads.

largest features in the anisotropy function (Fig. 2.b) and of the correction functions is striking. The correction function average amplitudes are down from anisotropy average amplitudes by factors of 8.1, 2.9 and 1.7, while the average phases are similar.

Fig. 3 shows RA-DEC significance maps before and after the correction is applied. The correction flattens the sky. Comparing Fig. 3(b) and 2(a) we see that the remaining high significance bins near $RA = 300^{\circ}$ are in the inner galaxy.

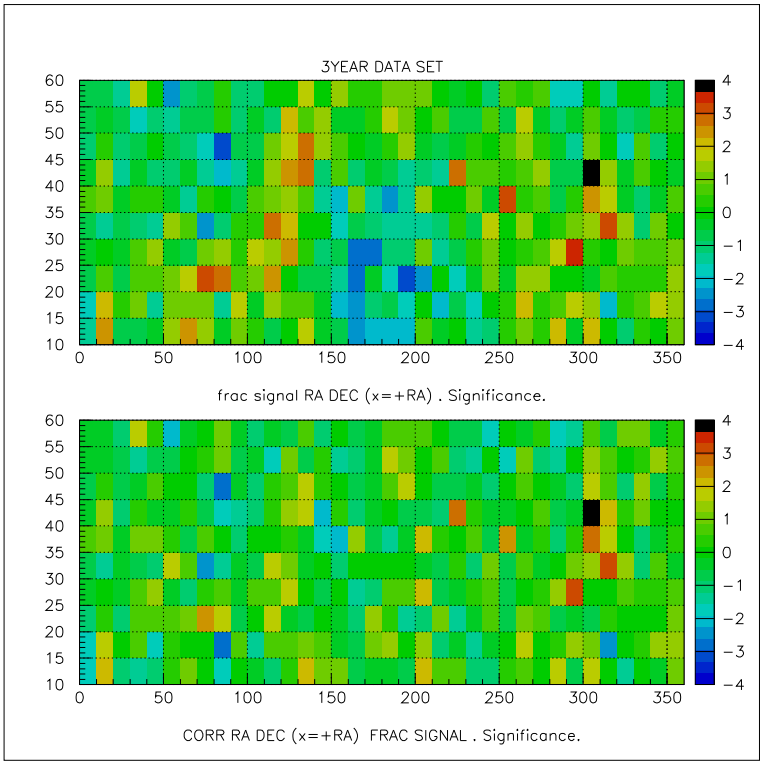

Fig. 3. RA-DEC Significance maps before and after IGEX bgnd. corr.

Fig. 4 shows the galactic coordinate significance maps before and after the correction. Again, the large scale structure largely disappears, while the Inner Galaxy ridge survives. The gaussian fit of the significance distributions of Fig.5(a) and (b) has $\sigma = 1.39$ before the correction going to $\sigma = 0.98$ after the correction. Fig.5(c) excludes the inner galaxy bins from the corrrected significance distribution.

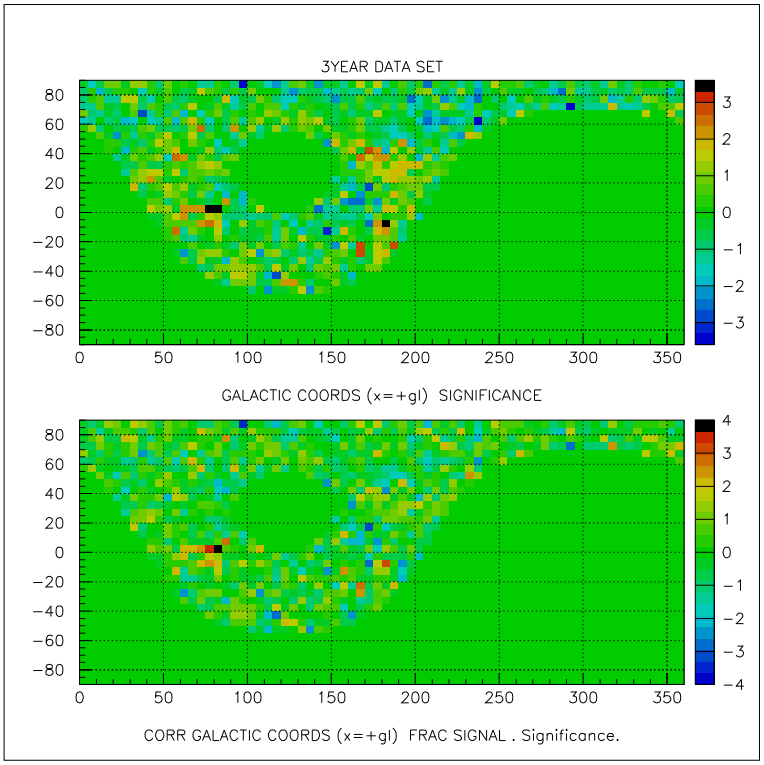

Fig. 4. Gal. significance maps before and after IGEX bgnd. corr.

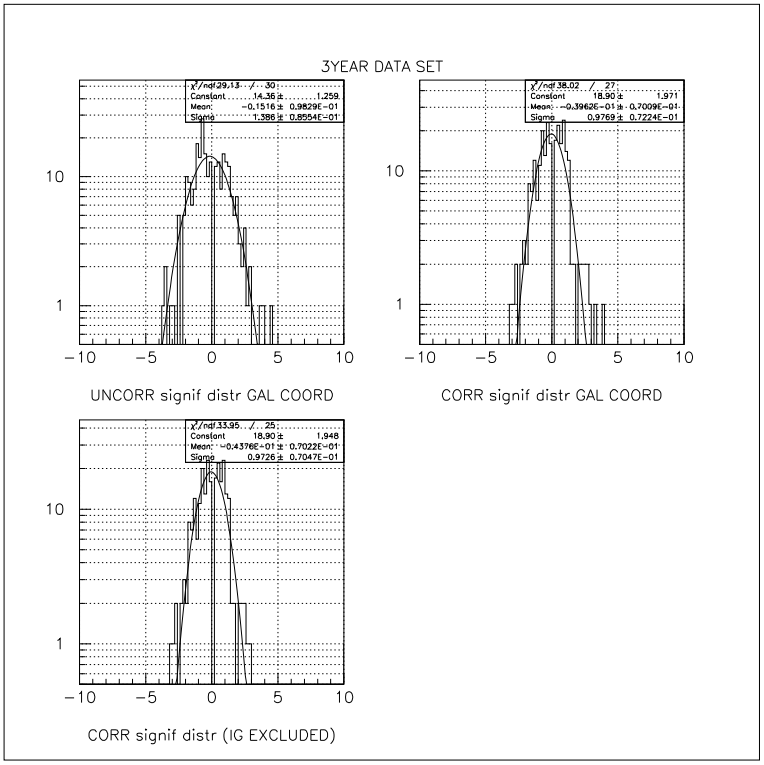

Fig. 5. Gal. signif. distr. without/with IGEX bgnd. corr, and IG bins excluded.

Fig. 6 gives the galactic equator longitude profile, and Fig. 7 the inner galaxy region latitude profile, before and after correction.

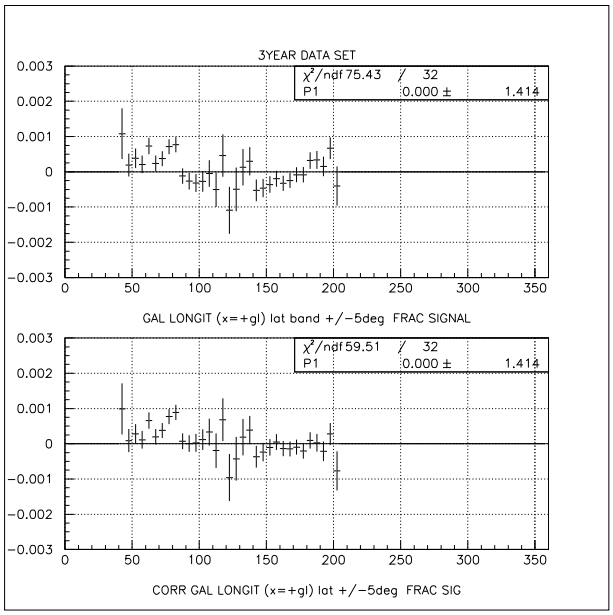

Fig. 6. Gal. coord. Equator Longit. Profile without/with IGEX bgnd. corr.

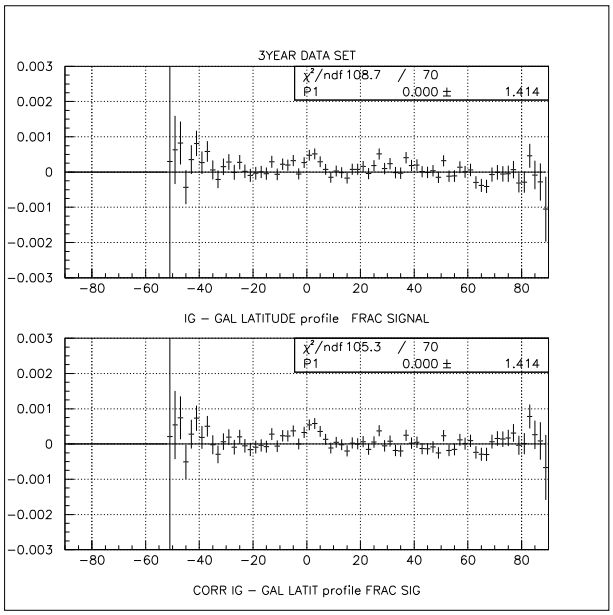

Fig. 7. IG region Gal. coord latitude profile without/with IGEX bgnd. corr.

The fractional background correction to subtract from the single bin Inner Galaxy result, $-0.70 \cdot 10^{-4}$ (IG-OG ex.) and $-0.61 \cdot 10^{-4}$ (IG only ex), is not sensitive to the choice of exclusion.

Fig. 8 shows the variation of the correction for a $\pm 1\sigma$ change of each of the parameters from their fitted values, while keeping the others at the fitted value. We assign a systematic error of $\pm 0.25 \cdot 10^{-4}$ as a reasonable match for the variations, and make the IGEX background correction of

$$\delta = (-0.61 \pm 0.25(syst)) \cdot 10^{-4},$$

to get a corrected fractional excess of:

$$FR = (3.54 \pm 0.73(stat) \pm 0.25(syst)) \cdot 10^{-4}.$$

The confidence level is 4.85σ using the statistical error, or 4.59σ using the combined error. [2].

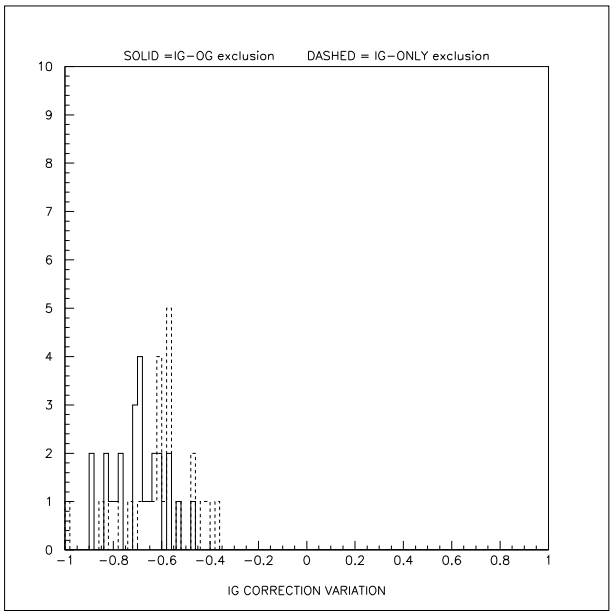

Fig. 8. Single bin IG bgnd. correction variation.

5 Systematics: Consistency Checks.

5.1 Anti X2 Analysis.

On the hadron side of the X2 cut we expect a suppressed, but nonzero fractional signal, compared to the gamma side. With a nine-fold increase of the background and 55% of the gamma signal on the anti-X2 side, we estimate a suppression factor of 7.4 (Ref. 4), predicting a fractional signal of $FR(expected) = 0.5 \cdot 10^{-4}$ for the anti-X2 data.

[2]Combination in quadrature since systematic error also has a statistical origin.

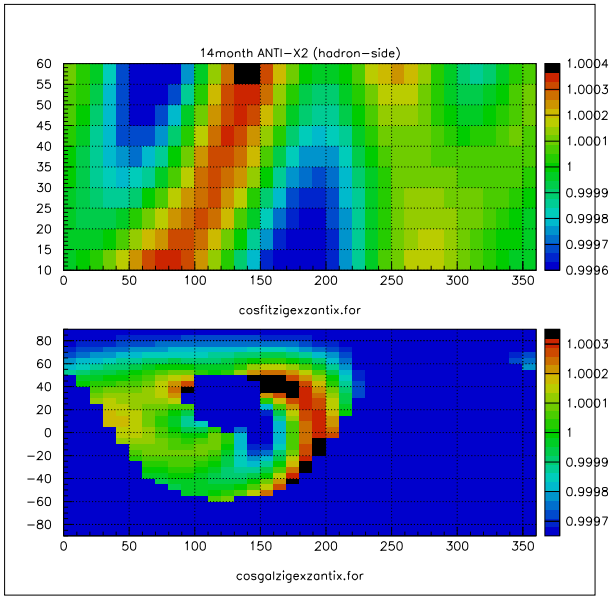

Fig. 9. IGEX Correction Function for anti-X2 data.

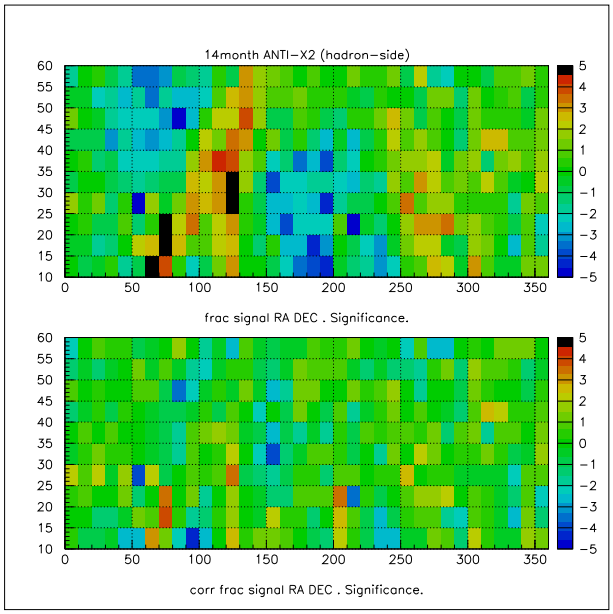

Fig. 10. Anti-X2 RA-DEC signif. map without/with IGEX bgnd.corr.

We have performed an analysis identical to that of the X2 cut data, including the background correction, on a 14month sample of the anti-X2 data (the sample size is three times that of our three year data set with the X2 cut). The 12 paramater background fit (for exclusion choice IG) is shown in Fig. 9; Fig. 10. shows the RA-DEC significance map before and after the correction. Fig. 11 and 12 display the significance maps and significance distributions in galactic coordinates, before

and after correction. The large-angular-scale modulation is well visible before the correction, but not after it. The (σ) of the gaussian fit to the significance distribution goes from 1.57 to 1.07.

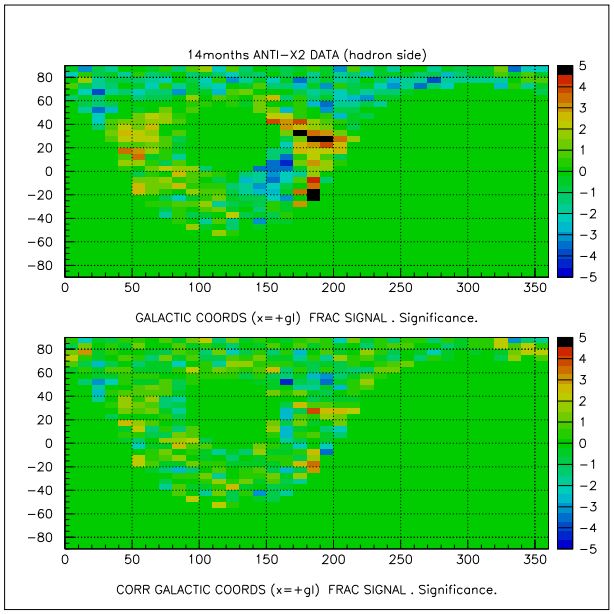

Fig. 11. Gal Signif. Map(anti-X2) without/with IGEX bgnd.corr.

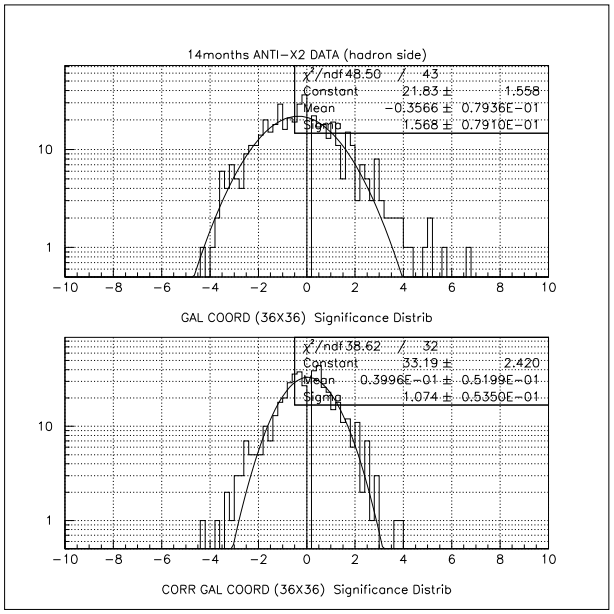

Fig. 12. Gal Signif. distribution(anti-X2) without/with IGEX bgnd.corr.

Before correction the IG signal is $FRAC = (1.35 \pm 0.53) \cdot 10^{-4}$. The IG single bin background correction is $0.61 \cdot 10^{-4}$(IG-only exclusion) or $0.48 \cdot 10^{-4}$ (IG-OG exclusion). The corrected IG

fractional signal of $FRAC = (0.74 \cdot \pm 0.53)10^{-4}$ or $FRAC = (0.87 \pm 0.53) \cdot 10^{-4}$ in good agreement, for either choice, with the expected one from the first paragraph.

5.2 Outer Galaxy.

The region around the OG has larger and more complicated corrections than the region around the IG (see Fig. 2 and 9). Figs. 13 shows the OG region latitude profile for X2 cut data. The correction somewhat improves this region.

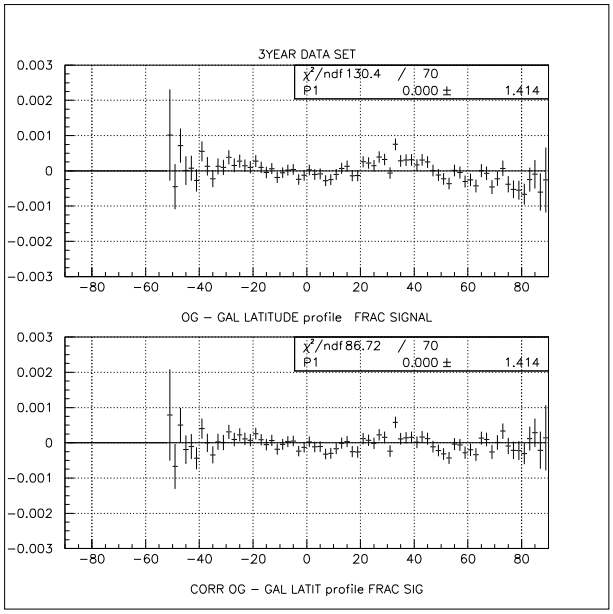

Fig. 13. OG region Gal. coord latitude profile without/with IGEX bgnd.corr.

For anti-X2, the OG single bin fractional signal is $FRAC = (-1.55 \pm 0.52)10^{-4}(-3\sigma)$. After the correction it is $FRAC = (-1.12 \pm 0.52) \cdot 10^{-4}(-2.1\sigma)$ for exclusion choice IG-OG and $FRAC = (-0.60 \pm 0.52) \cdot 10^{-4}(-1.1\sigma)$ for exclusion choice IGEX.

On the X2-cut gamma side data, the OG single bin fractional signal is $FRAC = (-1.01 \pm 0.73) \cdot 10^{-4}$ before the correction and

$FRAC = (-1.04 \pm 0.73) \cdot 10^{-4}(-1.42\sigma)$ after the correction.

Fig. 14 shows a much larger variation of the OG correction for a $\pm 1\sigma$ change of all the parameters from their fitted values, than Fig.7 did for the IG. Therefore, we assign a systematic error of $\pm 0.50 \cdot 10^{-4}$, and get for the OG:

$FRAC = (-1.04 \pm 0.73(stat) \pm 0.50(syst)) \cdot 10^{-}4$

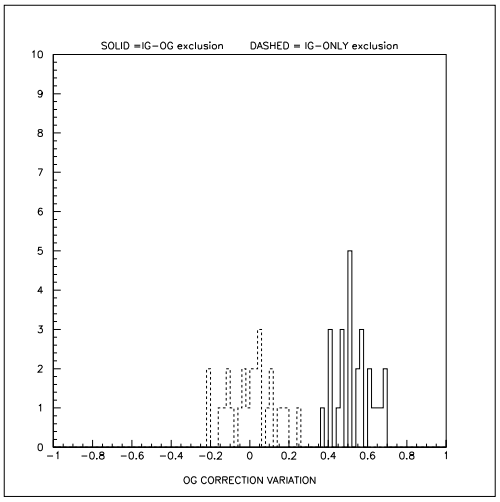

Fig. 14. Single bin OG bgnd. correction variation.

5.3 Zenith Breathing Correction.

The typical size of the Zenith breathing correction was seen to be about $0.5 \cdot 10^{-4}$ in a study turning it on and off on 14months of data (Ref.4).

As seen in the examples of Fig. 15, the zenith breathing correction-functions for data with no dec cut are different from those with the dec cut. Redoing the basic dec-cut analysis with the wrong, no-dec cut correction functions changes the IG single bin fractional signal by $\delta = -0.10 \cdot 10^{-4}$. We estimate that fit uncertainties in the correct fit are less by a factor of 3 than the differences seen in Fig. 15. We conclude that at a level of about $0.03 \cdot 10^{-4}$ the systematic error of the breathing correction is negligible.

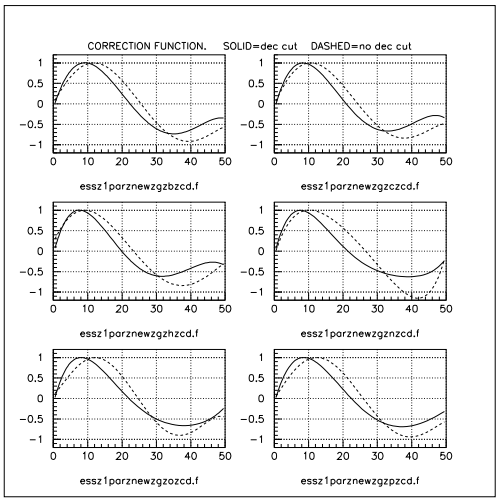

Fig. 15. Single bin OG bgnd. correction variation.

6 From Fractional Signal to Galactic Plane Flux .

6.1 The Case for Using Fractional Signal .

Starting with the FRAC signal, excess/cosmic-background, rather than total number of observed events, eliminates the difficult task of having to keep detailed track of all inefficiencies, such as hardware(ems) deadtime, time-off interruptions, varying (and possibly unknown) losses both in hardware and software (beyond the ems deadime), the bad runs and bad-data thrown away(see section 2), the event loss from imposed cuts, trigger efficiency and the nonnegligible changes of event rate (threshold) during three years of running. All of these things affect background and excess in same way, and therefore cancel in the fractional signal FRAC. Working with the absolute number of events, on the other hand, any neglected inefficiency would be one sided bias leading always to an underestimation of flux.

Working with the FRAC signal also reduces our sensitivity to abolute energy scale from the steep power-law coefficient of the energy distribution to a much less steep difference between the hadron and gamma power law coefficient. Finally, the FRAC signal gives us the right currency to compare one analysis to another, with non-identical methods, cuts and data sets, or compare the behavior of subsets of the data.

There is a price to pay: more needed input from MC simulations of effective area(EA). Instead of needing only EA(gamma), we need the ratio EA(gamma)/EA(cr). Here too there may be some cancellation by the ratio of some common bias. On the other hand any systematic error or bias specific to the hadron Monte-Carlo will affect the result. If we suspect or know of biases, we need to estimate them and shift the answer; if we expect larger uncertainties in the hadron monte carlo than in the gamma one, we must increase the assigned systematic error accordingly.

6.2 Integral Flux Ratio: Galactic Signal/Cosmic Rays.

Although most of our cosmic ray triggers come from protons, helium is also a major component of the primary cosmic rays. Throughout the following we'll use the symbol ϕ for the integral flux above 1TeV energy/nucleus, in units of $cm^{-2}ster^{-1}sec^{-1}$. From balloon data by JACEE (Ref.5) $\phi(P) = 0.62 \cdot 10^{-5}$ and $\phi(He) = 0.48 \cdot 10^{-5}$. The sum of the two fluxes $\phi(P+He) = 1.1 \cdot 10^{-}5$ is in good agreement with the satellite measurement of total integral flux by Grigorov (Ref.6), $\phi(cr) = 1.2 \cdot 10^{-5}$ From the above, the helium fraction is $\phi(He)/(\phi(He)+\phi(P)) = 44\%$.

Bob Ellsworth has done a detailed study of He vs P in his note "Monte Carlo Simulations of Milagro Trigger Rates" (Ref.7) on which we rely here. For triggers without an X2 cut, the conclusion that our Helium triggers are about 25% of the Proton triggers, together with the Flux ratio above, translates to $EA(He) = EA(P)/3$, where EA is the effective area integrated over energy. Triggers from heavier nuclei are negligible. Also from Monte Carlo data provided by Bob, the X2 distribution is narrower for He than for Protons with the fraction passing the X2 cut at 7.0% in He versus 9.6% in P. This gives $EA(He,X2) = EA(P,X2)/4.1$

From Fig. 11.4 of RF thesis (Ref.1), with the X2 cut and averaged over the transit of the IG, the Milagro energy integrated effective area ratio of gammas to protons (for an assumed power law

coeff. $\alpha(\gamma) = 2.7$) is $\eta = 4.5$.

Combining all this, we can write:

$$FRAC = TRIG(\gamma)/TRIG(cr) = \phi(\gamma)EA(\gamma)/(\phi(P)EA(P) + \phi(He)EA(P)/4.1),$$

that is

$$FRAC = \phi(\gamma)/(\phi(P+He)/\eta', \text{ where } \eta' = 4.5/(56\% + 44\%/4.1) = 6.74$$

After consulting with Bob, we assign a 50% systematic error to the He to P EA ratio. We assign an additional 25% systematic error to the proton EA, based on the discrepancy between the (6/24/01) data rate and the MC sum of He + P rate in the next to last Figure of Bob's note, evaluated at nfit=25. The Monte Carlo over-estimates the trigger rate. If the discrepancy is due to a problem specific to the hadron MC, we should adjust η' by 25% if it is a common problem of the hadron and gamma MC, we should not. Since we do not know which, a priori, we make an adjustment by half this amount, 12.5%, giving $\eta' = 7.58$

In addition we make the assumption of the Crab paper, a possible 20% systematic error in energy scale, but propagate it with the difference between power law indices $(\alpha(\gamma) - \alpha(P)$, taken as no bigger than 0.3, to get a max energy scale induced systematic error of 6% Propagating and combining all the above errors (in quadrature) gives

$$\eta' = 7.58 \pm 2.11(syst)$$

and therefore a flux ratio

$$RFLUX = \phi(\gamma)/(\phi(He+P) = FRAC/(7.58 \pm 2.11(syst))$$

yielding a gamma flux to cosmic flux ratio of

$$RFLUX = \phi(\gamma)/\phi(He+P) = (4.67 \pm 1.63) \cdot 10^{-5},$$

where all errors are combined in quadrature. [3] We note that the error above mixes the scale error with the original discovery error; the larger fractional error here is not a decrease of the significance of the discovery.

The IG single bin analysis is equivalent to an assumption that the source signal distribution is flat for the IG region. For a projected angular resolution of $\sigma = 0.75^\circ$ there is a loss of 5.1% of reconstructed events leaking out of the $\pm 5^\circ$ IG analysis region. Correcting for this leakage, the flux ratio becomes:

$$RFLUX = \phi(\gamma)/\phi(He+P) = (4.92 \pm 1.72) \cdot 10^{-5},$$

A reasonable alternative assumption is that the longitudinal source signal distribution in our IG window is the same as Egret's (Ref.8.). Fitting the Egret source distribution (ESD) in Fig. 16 gives

[3] The value PN provided for SAGENAP, $8.1 \cdot 10^{-5}$, was an overestimate because it assumed all cr are protons, neglecting the lower effective area for Helium. This is an example of a hadronic bias that needed correcting.

an average fractional signal that is about 25% higher. The resolution leakage is negligible for an Egret-like transverse profile; no leakage correction is made.

$FRAC(ESD) = (4.64 \pm 0.87(stat) \pm 0.25(syst)) \cdot 10^{-4}$.

and a corresponding flux ratio

$RFLUX(ESD) = \phi(\gamma)/\phi(He+P) = (6.12 \pm 2.09) \cdot 10^{-5}$.

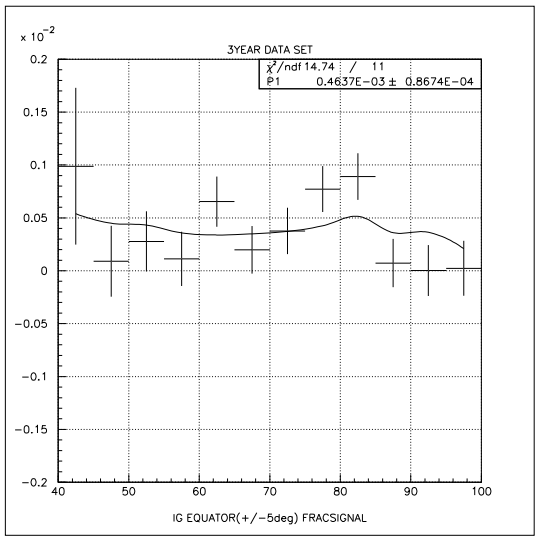

Fig. 16. IG region fit to EGRET source distribution (ESD).

6.3 Integral Flux from Inner Galaxy.

We can now obtain the average flux for our gamma signal from our IG region (for either assumption) by multiplying the flux ratio by the sum of P and He fluxes from JACEE (at 1TeV) $\phi(He) + \phi(P) = 1.1 \cdot 10^{-5}$ to get our final experimental answer.

The Integral-Flux for $E > 1.0TeV$ [4] of observed diffuse gamma emission in the Milagro inner Galaxy (IG) region is, for $\alpha(\gamma) = 2.7$:

$\phi(E > 1.0TeV) = (5.4 \pm 1.9) \cdot 10^{-10}(ster^{-1}cm^{-2}sec^{-1})$

for a flat source distribution, or

$\phi(E > 1.0TeV, ESD) = (6.7 \pm 2.3) \cdot 10^{-10}(ster^{-1}cm^{-2}sec^{-1})$

for an Egret-like source distribution.

[4] We are sensitive to this choice to represent the Milagro threshold only by the difference of cosmic ray and gamma power law cofficients.

For a different power law coefficient $\alpha(\gamma)$ the results can be scaled with $1/\eta$) from Fig. 11.4 of Ref.1. We tabulate them here for a few values of $\alpha(\gamma)$:

$\alpha(\gamma)$	Flat Source Distr.	Egret Source Distr.
2.5	$(4.8 \pm 1.7) \cdot 10^{-10}$	$(5.9 \pm 2.0) \cdot 10^{-10}$
2.6	$(5.1 \pm 1.8) \cdot 10^{-10}$	$(6.4 \pm 2.2) \cdot 10^{-10}$
2.7	$(5.4 \pm 1.9) \cdot 10^{-10}$	$(6.7 \pm 2.3) \cdot 10^{-10}$
2.8	$(5.6 \pm 2.0) \cdot 10^{-10}$	$(7.0 \pm 2.4) \cdot 10^{-10}$
2.9	$(5.7 \pm 2.0) \cdot 10^{-10}$	$(7.1 \pm 2.4) \cdot 10^{-10}$

Table I. Integral Flux($E > 1TeV$) versus power law coeff.($ster^{-1}cm^{-2}sec^{-1}$)

6.4 Egret Milagro Comparison.

Fitting the top 4 energy points of the Egret differential distribution (1GeV to 30geV) in Fig. 17, restricted to the region of the Milagro Inner galaxy (IG), yields a power law spectral index of $\alpha = 2.53 \pm 0.01$. This index is somewhat softer than that in the Egret innermost galaxy around the galactic center.[5]

[5] An alternate way of fitting the same region gave an estimate of $\alpha = 2.45 \pm 0.05$.

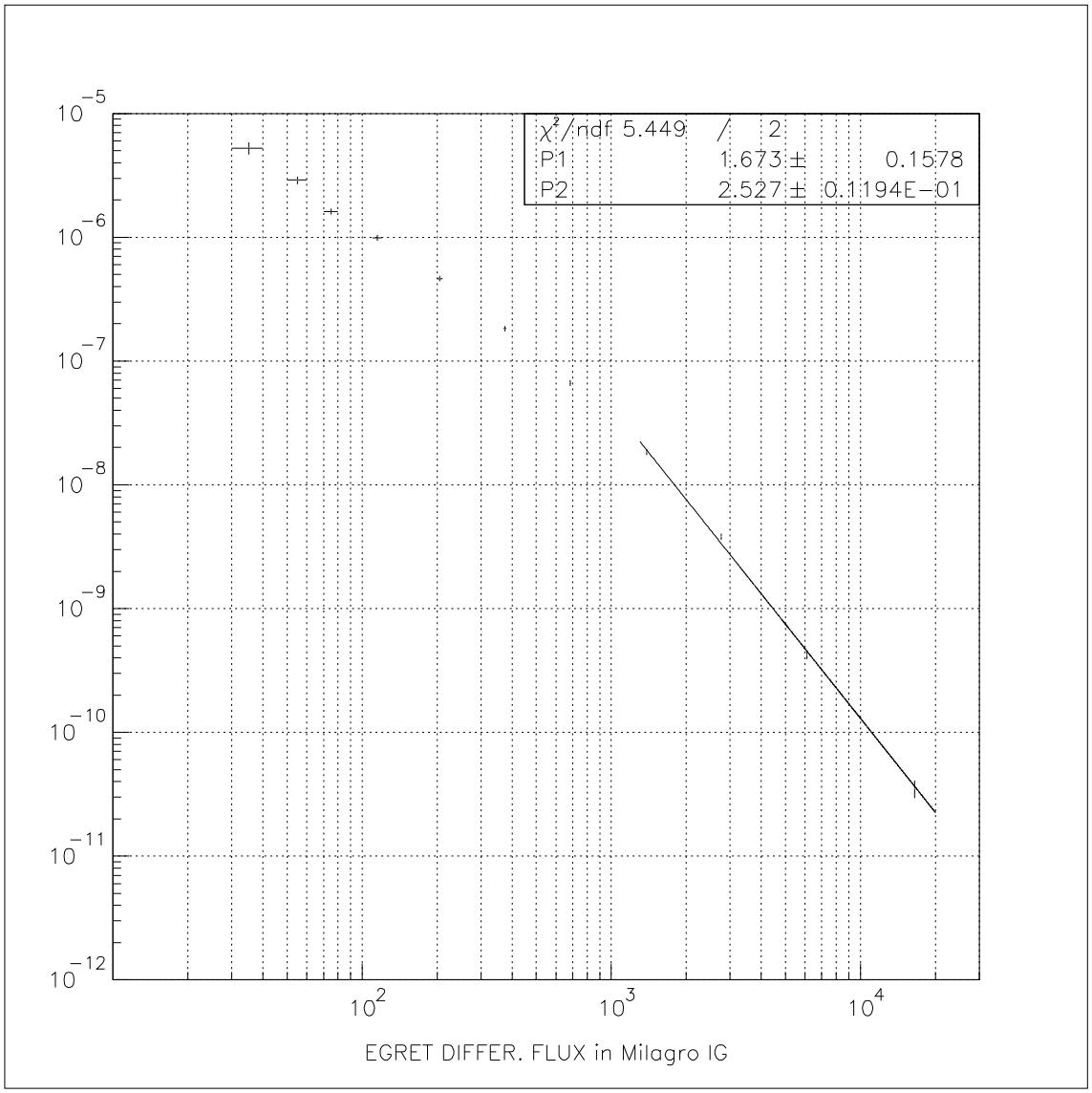

Fig. 17. Egret Differential Flux in Milagro IG region.

Because our Milagro result is in a fact a single measurement of integral flux, we display the Milagro and Egret results together as integral fluxes in Fig. 18.

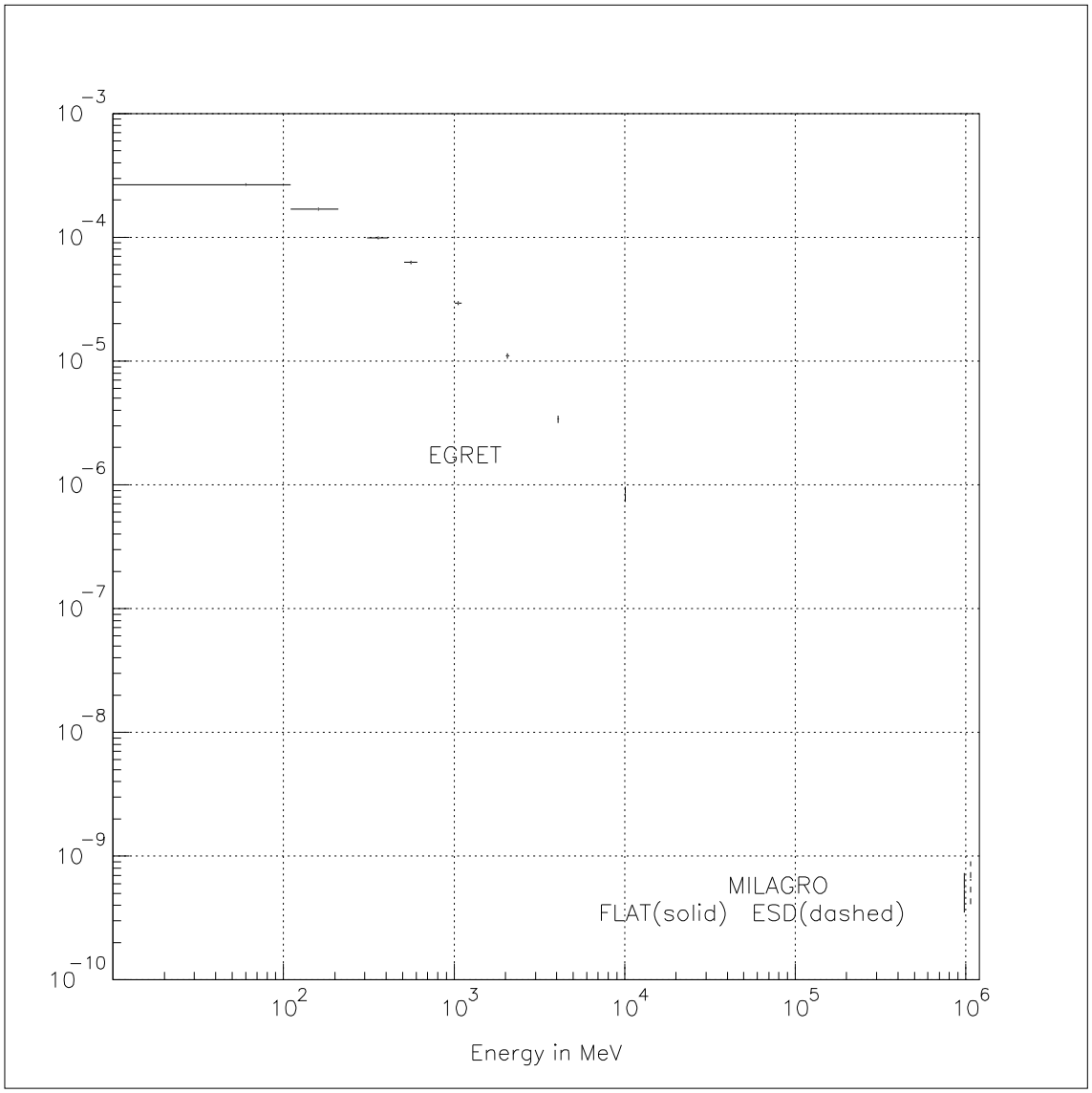

Fig. 18. Egret and Milagro Integral Flux in IG region ($cm^{-2}ster^{-1}sec^{-1}$).

The assumption that there is a single power law with no "knees" from EGRET'S high end through the Milagro energies, provides the constraint to translate our Milagro integral cross-section result into the common power law coefficient that is consistent with Milagro and EGRET. The results are

$\alpha = 2.70 \pm 0.08$ for a flat source distribution,

and

$\alpha = 2.66 \pm 0.08$ for an Egret-like source distribution (ESD).

In our Milagro IG region these power law coefficients are softer than EGRET's high end one by 2.1σ or 1.6σ for a flat and ESD source, respectively.

As an alternate display, we translate our Milagro integral flux to a differential flux, and replot in Fig. 19 the Egret and Milagro data as Energy-squared times the differential flux. [6]

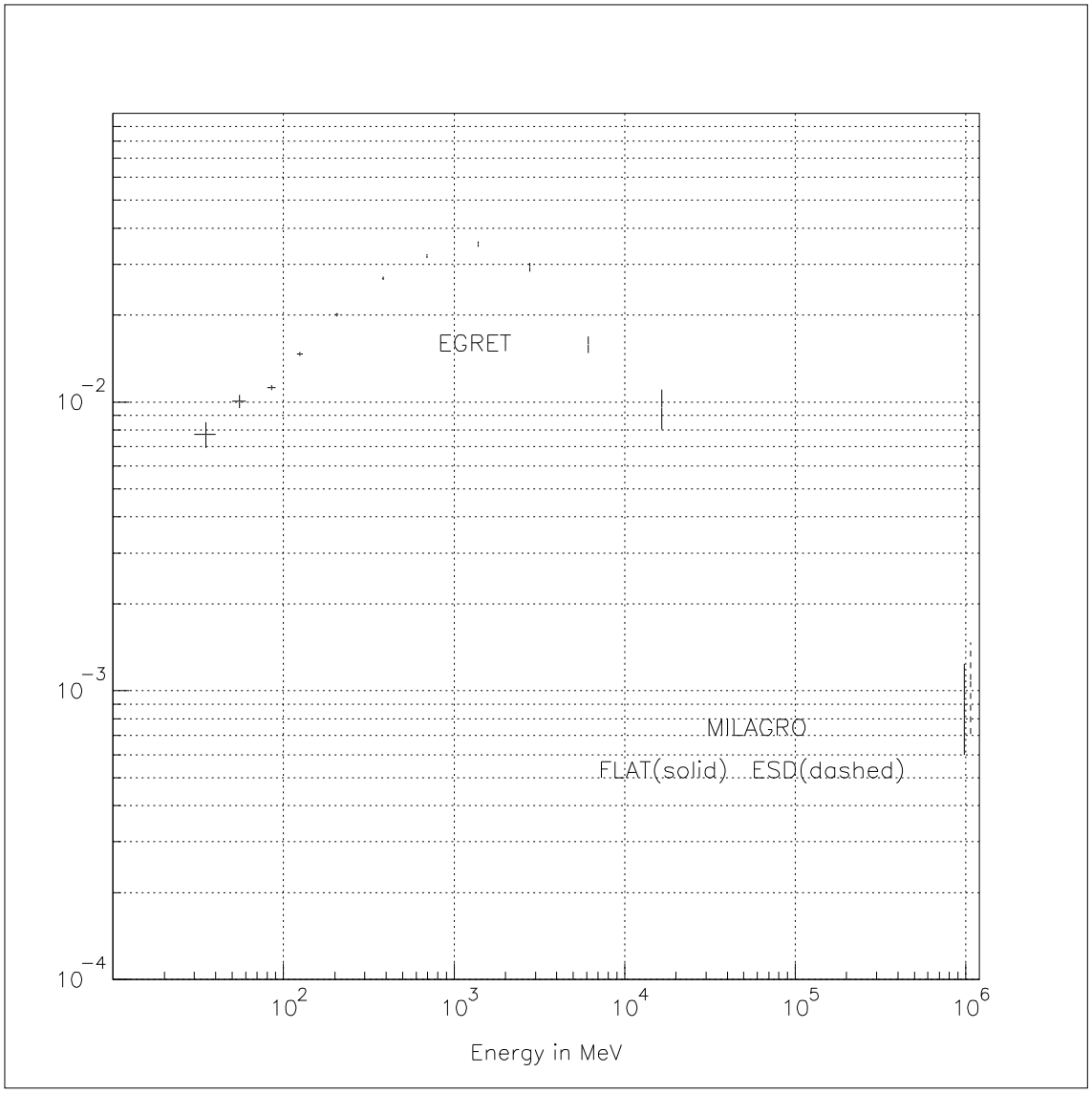

Fig. 19. $E^2 \cdot dN/dE$ in IG Region ($cm^{-2}ster^{-1}sec^{-1}MeV$).

7 Acknowledgment.

We thank Bob Ellsworth and Brenda Dingus for useful discussions.

[6] In both Fig. 18 and Fig. 19 we display the results with α-s from the single power law constraint.

References.

1. "Search for Gamma Ray Emission from Galactic Plane with Milagro." Roman Fleysher. Dissertation submitted in partial fulfillment of the requirements of the degree of Doctor of Philosphy. New York University, 2003.

2."Tests of Statistical Significance and Background Estimation in Cosmic Ray Air Shower Experiments." R. Fleysher, L. Fleysher, P. Nemethy, A. I. Mincer and T. J. Haines. Ap. J. 603, 355 (2004).

3. Galactic Plane & Cosmic Ray Anisotropy." P. Nemethy. Presentation at Milagro Collaboration Meeting, Asilomar, Nov. 2003.

4. "Galactic Plane: Anti-X2 Study" P. Nemethy. Presentation at Milagro Collaboration Meeting, UMd, Mar. 2003.

5. K.Asakamori et al. "Cosmic Ray Proton and Helium Spectra: Results from th JACEE Experiment. Ap. J. 502, 278 (1998).

6. N. Grigorov et al. Proc. 12-th ICRC, Hobarth Australia, 5 1746 (1971).

7. "Monte Carlo Simulations of Milagro Trigger Rates" R. Ellsworth.

$http://umdgrb.umd.edu/ellsworth/olderstuff/Trigger-Rates/$

8. S. D. Hunter et al., Astrophysical Journal 481, 205 (1997), and private communication.